Steroids 158 (2020) 108602

Contents lists available at ScienceDirect

Steroids

journal homepage: www.elsevier.com/locate/steroids

Biological activity and apoptotic signaling pathway of C_{11}-functionalized cephalostatin 1 analogues

Mansour M. Nawasreh[a], Elham I. Alzyoud[b,c], Zainab A. Al-Mazaydeh[b], Majdoleen S. Rammaha[b], Salem R. Yasin[b], Lubna H. Tahtamouni[b,d,*]

[a] Applied Sciences Department, Faculty of Engineering Technology, Al-Balqa Applied University, Amman 11134, Jordan
[b] Department of Biology and Biotechnology, Faculty of Science, The Hashemite University, Zarqa 13115, Jordan
[c] Department of Genetics, University of Szeged, H-6720 Szeged, Hungary
[d] Department of Biochemistry and Molecular Biology, College of Natural Sciences, Colorado State University, Fort Collins 80523, CO, USA

ARTICLE INFO

Keywords:
Cephalostatin 1 analogues
ER stress pathway
Caspase 4
Smac/DIABLO

ABSTRACT

Cephalostatin 1, a potent anti-cancer agent, is a natural bis-steroidal alkaloid that causes cell death in the subnanomolar to picomolar ranges via an atypical apoptosis pathway. Although cephalostatin 1 is a highly effective anticancer drug, its availability limits its utilization. We previously reported the synthesis of two 12′α-hydroxy derivatives of cephalostatin 1 that induce cell death by activating the ER stress apoptosis signaling pathway. For the current work, we synthesized six C_{11}-functionalized cephalostatin 1 analogues (CAs) to evaluate their biological activity. For the cytotoxic compounds, the induced apoptotic pathway was investigated. The C_{11}-functionalized cephalostatin 1 analogues **5** and **6** (CA5 and CA6) were found to exhibit cytotoxic activity against K-562 leukemia cells, MCF-7 breast cancer cells and DU-145 prostate cancer cells, while the remaining four analogues did not show anti-tumor activities against any of the cell lines. Our results indicated that CA5 and CA6 induced cell death via the atypical ER-dependent apoptosis pathway; they increased the expression of Smac/DIABLO, an inhibitor of inhibitors of apoptosis (IAPs), which in turn facilitated the activation of different caspases including the ER-caspase 4 without cytochrome *c* release from mitochondria. CA5 and CA6 are promising anticancer agents due to their low GI_{50}, the remarkable apoptosis pathway they induce which can overcome chemoresistance, and their very low toxicity to normal cells making them cephalostatin 1 utilizable alternatives.

1. Introduction

The discovery of different chemotherapeutic drugs has opened a new era for the treatment of multiple cancers. However, the efficiency of most antitumor drugs is often accompanied by toxic side effects and tumor chemoresistance, which in turn leads to relapse [1,2]. The classical anticancer agents are the alkylating agents, anti-metabolites, topoisomerase inhibitors and tubulin-acting agents (mitotic inhibitors) [3–5]. However, there is still a need for developing effective anticancer drugs with more specific action against tumor cells without affecting normal tissues [6], as well as having new mechanisms of action such as growth factors, signaling molecules, cell-cycle proteins, modulators of apoptosis, and molecules that inhibit angiogenesis.

Genetic and biochemical studies have identified two major pathways of apoptosis: the extrinsic pathway (mitochondria-independent, death receptor-mediated pathway) and the intrinsic pathway (mitochondria-dependent pathway). Both pathways converge at a specific level of caspase cascade [7]. The extrinsic pathway is induced by binding of specific death ligands with their transmembrane death receptors which results in quick activation of caspase 8 [8]. This in turn activates downstream effector caspases such as caspase 7, 6 and 3 that mediates the execution phase of apoptosis with a cascade of proteolytic activity within the cell.

The key event of the intrinsic pathway is mitochondrial outer membrane permeabilization (MOMP) which results in the release of mitochondrial intermembrane proteins such as cytochrome *c*, second mitochondria-derived activator of caspase/direct IAP (Inhibitor of Apoptosis Proteins) binding protein with low isoelectric point (Smac/DIABLO), apoptosis inducing factor (AIF) and endonuclease D (EndoD) into the cytosol [9]. Cytosolic cytochrome *c* binds to ATP, apoptosis-protease activating factor 1 (Apaf-1) and procaspase 9 to form a complex known as apoptosome which activates procaspase 9. In turn,

* Corresponding author.
E-mail addresses: lubnatahtamuni@hu.edu.jo, ltahtamo@colostate.edu (L.H. Tahtamouni).

https://doi.org/10.1016/j.steroids.2020.108602
Received 1 December 2019; Received in revised form 7 January 2020; Accepted 27 January 2020
Available online 22 February 2020
0039-128X/

caspase 9 can then activate downstream effector caspases such as caspase 3 [10]. Smac/DIABLO inhibits the action of IAPs [11].

Many studies implicated a regulatory role for the endoplasmic reticulum (ER) in apoptosis. The ER under stress initiates its own apoptotic signals, and has its own complement of apoptotic accessories that independently activate caspases [12]. The ER has a specific stress response that senses the shortage of Ca^{2+} within the ER, over production of proteins and accumulation of unfolded proteins [12,13]. ER stress response activates expression of ER chaperones and initiates signaling of the unfolded protein response, which inhibits protein synthesis through phosphorylation of the eukaryotic translation initiation factor 2 (eIF2) and facilitates protein degradation [12,14].

Severe ER-stress has the ability to induce apoptosis through a mitochondria- independent pathway. Caspase 4, the main player in the ER-dependent apoptosis, is synthesized and localized to the ER membrane. After being activated, caspase 4 cleaves and activates caspase 9 independently of cytochrome *c* and Apaf-1; caspase 9 in turn activates caspase 3 [15]. ER-stress also might provide a pathway for the accumulation of Smac/DIABLO which in turn inhibits IAP contributing to the activation of caspases [12].

Cephalostatin 1 is a member of structurally related bis-steroidal compounds (cephalostatins 1–20) which were identified and isolated from extracts of the tunicate *Cephalodiscus gilchristi*, a small Southeast African marine worm. Cephalostatin 1, the most active member, was reported to have an anti-proliferative activity in the range of sub-nanomolar to picomolar concentrations [16,17]. In addition, cephalostatin 1 induces apoptosis through the ER-mediated pathway independent of cytochrome *c* release and caspase 8 activation, and it selectively uses Smac/DIABLO as a mitochondrial signaling molecule [16]. This in turn gives cephalostatin 1 the ability to overcome chemoresistance [18].

However, the availability of cephalostatin 1 from its natural source is extremely limited (138.38 mg out of 166 kg tunicate, $8.4x10^{-7}$ yield (w/w), [19]) and its total synthesis was found to be very complicated [more than 65 steps with about 1–9 $\times$ 10^{-4} overall yield (w/w) from hecogenin acetate] [20,21]. Combination of its lack of availability along with its exceptional anti-proliferative activity led to a strong interest in the synthesis of cephalostatin 1 analogues (cephalostatin 1-related compounds) as potential antitumor agents, and to evaluate their biological activities looking for utilizable alternatives to cephalostatin 1 [22–28].

Previously, our group reported the synthesis of two 12′α-hydroxy derivatives of cephalostatin 1 and their ability to induce cell death by activating the atypical ER stress apoptosis signaling pathway [28]. As part of our continuous investigation into developing active synthetic analogues of cephalostatin 1, we modified position C-11 by functionalization with an -OX group (X = Me, Et, H) of the bis-steroidal dimer **2** (Schemes 1, 2). Six cephalostatin 1 analogues that have an –OR or –OH functionality at C-11 were synthesized and their anti-tumor activities were evaluated in order to further understand how their biological activity would vary. This in turn should help in designing and synthesizing more powerful tumor inhibitory drugs.

2. Experimental

2.1. Compounds

Caspase 4 inhibitor (Ac-LEVD-CHO), etoposide (ET), diacetoxy iodobenzene ($PhI(OAc)_2$), sodium borohydride ($NaBH_4$), absolute ethanol and isopropanol (HPLC grade) were purchased from Sigma-Aldrich (MO, USA), broad spectrum pan-caspase inhibitor (benzyloxycarbonyl-Val-Ala-Asp(OMe)-fluoromethlketone; zVAD-fmk) was purchased from Bachem Americas, Inc. (CA, USA), thapsigargin (TG) was purchased from LC Laboratories (MA, USA). The bis-steroidal diketone (compound **2**, Scheme 1) was synthesized in our laboratory using standard procedure [29].

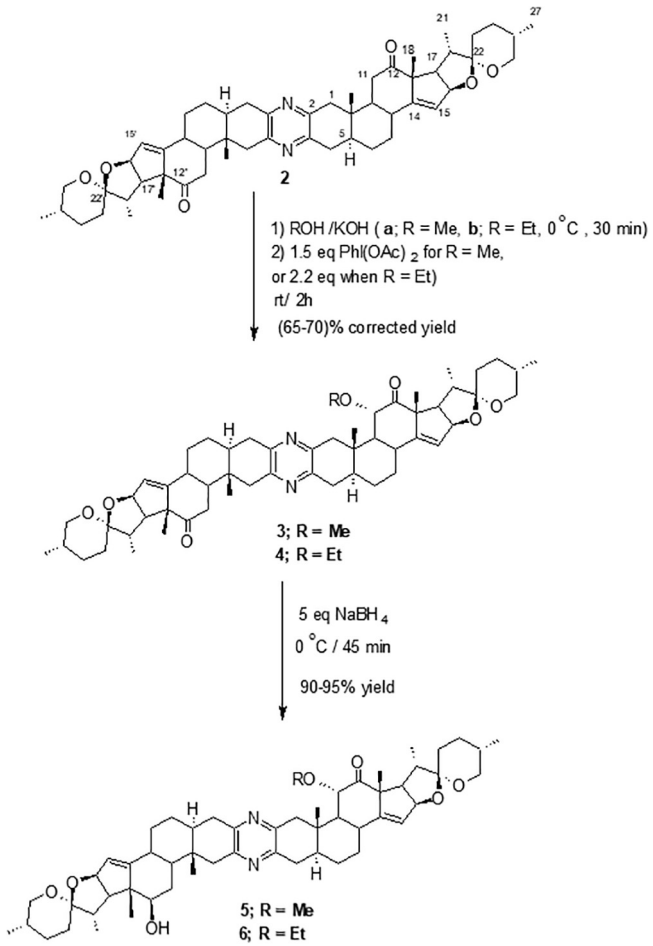

Scheme 1. Alkoxylation of position-11 of **2** followed by reduction with $NaBH_4$.

2.2. Synthesis and analysis methods of cephalostatin analogues

2.2.1. Preparation and characterization of compounds 3, 4 and 7

To prepare the three analogues (**3**, **4** and **7**), the following standard procedure was followed using as alcohols methanol (**3**), ethanol (**4**) and isopropanol (**7**). To a solution of 0.08 g of KOH in the 3 mL of the appropriate alcohol (MeOH, EtOH and i-PrOH) in 50 mL dry round bottom at 0 °C, a solution of the diketone **2** formed from 0.21 g (0.249 mmol, 1 eq) in 3 mL of dichloromethane was gradually added and stirred for 30 min. The resulting yellowish enolate solutions of the substrate was then treated with diacetoxy iodobenzene $PhI(OAc)_2$ (0.120 g (1.5 eq), 0.176 g (2.2 eq) and 0.241 g (3.0 eq) respectively, depending on the alcohol type) and stirred at room temperature for two hours (Schemes 1 and 2). Each reaction mixture was extracted between brine solution and dichloromethane twice. The resulting crude material of each reaction was chromatographed on a silica gel column and eluted with a gradient of ethyl acetate: petroleum ether mixture (EA/Pt) increasing from 5 to 50% EA. Each one of the three compounds **3**, **4** and **7** was characterized using NMR and MS spectroscopic techniques. The MS spectrum of compound **3** showed a molecular ion peak [MH^+] at *m/z* 875 as a base peak (formula $C_{55}H_{74}N_2O_7$), the structure of compound **3**, was confirmed from the ^1H NMR spectrum by the appearance of a sharp singlet resonating at 3.73 ppm corresponding to the methoxy group (–O<u>C</u>H_3). In addition, its ^{13}C NMR spectrum showed that the carbonyl carbon adjacent to the methoxy group (δ 174.6 ppm) is shifted up-field by about 36 ppm compared to its unmethoxylated counterpart (δ 210.9 ppm). A similar feature was noticed in ^{13}C NMR for the carbonyl carbon of the ethoxy compound **4**. Additionally, the existence of the ethoxy group appeared clearly in ^1H NMR which showed two multiplets

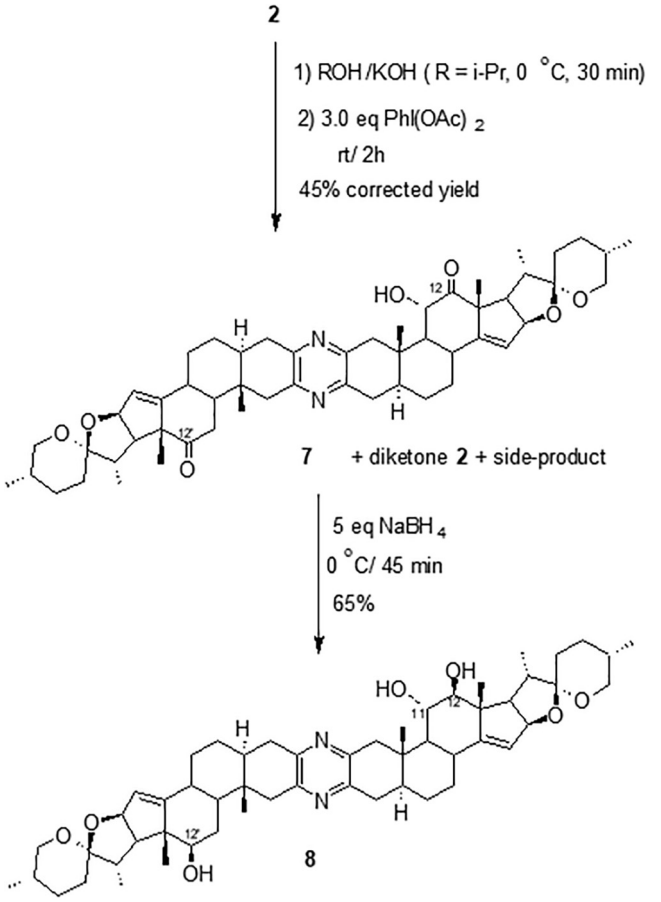

Scheme 2. Hydroxylation of position-11 of **2** followed by reduction with $NaBH_4$.

resonating at δ 4.26 and δ 4.10 ppm corresponding to the methylene protons (–O<u>CH</u>$_2$) of the ethoxy group. Moreover, the mass spectrum of compound **4** showed the molecular ion peak at *m/z* 889 [MH^+] as a base peak corresponding to the formula $C_{56}H_{76}N_2O_7$ which showed the additional ethyl group. The structure of compound **7** was deduced from the appearance of the molecular ion peak at *m/z* 861 (formula $C_{54}H_{72}N_2O_7$) corresponding to MH^+ ion as a base peak in its mass spectrum. In addition, the carbonyl group adjacent to the 11-hydroxy group resonates at δ 176.5 ppm compared to the carbonyl carbon in the other half which resonates at δ 210.7 ppm. Moreover, the IR spectrum of compound **7** showed the appearance of a broad peak at ν 3517 cm^{-1} corresponding to –OH group. This peak didn't appear in either compound **3** or **4**. The configuration of the hydroxyl group at C-11 was not specified in compound **7** due to its existence as a mixture of epimers.

2.2.2. Preparation and characterization of compounds 5, 6 and 8

After dissolving 60 mg of each of the compounds **3**, **4** and **7** in three separate flasks containing 4 mL of CH_2Cl_2/MeOH (1:1) mixture, each solution was cooled down to 0 °C. Each solution of compounds **3**, **4** and **7** was treated with 13 mg of $NaBH_4$ (about 5 eq) and stirred for 45 min at 0 °C each yielding a single major. The reaction mixture of each was quenched with 1 mL acetaldehyde and extracted between dichloromethane and brine twice. The collected organic phase was dried and the resulting crude material of each reaction was purified using silica gel column chromatography yielding the analogues **5**, **6** and **8** respectively (Schemes 1, 2). The structure of each purified analogue was deduced using different spectroscopic techniques such as ^{1}H NMR, ^{13}C NMR, MS and HR-MS. Since the three compounds **5**, **6** and **8** are sharing the left half of the dimer (Schemes 1 and 2), the ^{1}H NMR spectra of the three compounds showed the methine proton (C<u>H</u>OH) at C-12′ appearing as a multiplet resonating at δ 3.25 ppm. Moreover, the carbonyl group adjacent to the methoxy and ethoxy groups in both **5** and **6** respectively (Scheme 1) was protected against the sodium borohydride reagent which led to a chemoselective reduction. However, both carbonyl groups in **7** underwent reduction reaction leading to the triol **8** and hence chemoselectivity was lost (Scheme 2). This was noticed from the absence of any peak resonating at ν 1728 cm^{-1} in the IR spectrum of **8**. However, this peak still exists in both compound **5** and **6**. Moreover, the peak resonating at δ 175 ppm in the ^{13}C NMR of both compounds **5** and **6**, corresponding to C-12, remained as in their precursors **3** and **4**. Conversely, this peak disappeared from the spectrum of compound **8** when compared with its precursor **7**. Additionally, the mass spectrum MS (ESI) of compound **5** showed the peak at 877 as a base peak corresponding to MH^+ ion (formula: $C_{55}H_{76}N_2O_7$). For compound **6**, the base peak appeared at 891 for the MH^+ ion (formula: $C_{56}H_{78}N_2O_7$). However, for compound **8** the base peak appeared at 864 for corresponding for the M^+ ion (formula: $C_{54}H_{76}N_2O_7$).

2.3. Cell culture

Human K562 chronic myelogenous leukemic and human MCF-7 breast cancer cells were cultured in RPMI-1640 (Euroclone, Italy) supplemented with 10% fetal bovine serum (FBS; Capricorn Scientific, Germany). Human DU-145 prostate cancer cell line was cultured in α-MEM supplemented with 10% FBS. Trypsin-EDTA (Lonza, Switzerland) was routinely used for subcultures. Cells were grown at 37 °C in a humidified 5% CO_2/95% air atmosphere.

2.4. In vitro cytotoxicity (3-(4,5-Dimethylthiazol-2-yl)-2,5diphenyltetrazolium bromide) MTT test

MTT assay is a colorimetric cell viability assay [30]. CA stock solutions were prepared in 10% DMSO, such that the final DMSO concentration in culture did not exceed 0.1%. Cells were treated with CAs in 6 different concentrations: 0.005, 0.01, 0.05, 0.1, 1 and 10 μM and incubated for 24, 48 or 72 h. Freshly prepared MTT salt (final concentration 0.5 μg/ μl) was added for 4 h. Formazan crystal formation was checked on an inverted microscope and crystals were solubilized using a 1:1 mixture of DMSO and isopropanol. The inhibition of cell growth induced by the different CAs was detected by measuring the absorbance of each well at 570 nm using a Biotek Synergy HT Multi-Mode Microplate Reader (VT, USA). Percent growth was calculated according to the following formula: Growth (%) = OD treated/OD control × 100%. The concentration versus percent growth curve was used to calculate the concentration which caused 50% growth inhibition (GI_{50}) by linear interpolation, while the concentration that caused total growth inhibition (TGI) was read as the x-axis intercept.

2.5. Detection of apoptosis

The occurrence of apoptosis was detected by visualizing nuclei after staining with DAPI using a Nikon Eclipse Ti-E microscope and further confirmed by translocation of phosphatidylserine to the cell surface using annexin V-FITC apoptosis detection kit (Sigma, USA).

2.6. Clonogenic assay

2×10^5 cells were seeded in tissue culture dishes containing growth media supplemented with FBS and incubated at 37 °C for 24 h. Afterwards, the medium was replaced and the cells were incubated for 3 h in the presence of increasing concentrations (0.005, 0.01, 0.5, 0.1, 1, and 10 μM) of the different CAs. Aliquots of 1000 cells were seeded on soft agar [31] for MCF-7 and DU-145 cell lines, while K-562 leukemic cells were seeded on methylcellulose [32]. Cultures were incubated for 12 days. The colonies were then stained with crystal violet and counted, discarding colonies with < 50 cells. The surviving fraction

Table 1
Primer sequence and qRT-PCR reaction conditions for *caspase 3, 4, 8, 9, smac/DIABLO* and *β actin*.

Gene	Forward primer	Reverse primer	qRT-PCR conditions	Reference
caspase 3	TGGTTCATCCAGTCGCTTTG	CATTCTGTTGCCACCTTTCG	hold stage at 95 °C for 3 min, 40 cycles of PCR stage at 95 °C for 15 *sec*, 60 °C for 1 min and 72 °C for 30 *sec*	[34]
caspase 4	CAGACTCTATGCAAGAGAAGCAACGTATGGCAGGA	CACCTCTGCAGGCCTGGACAATGATGAC	hold stage at 95 °C for 15 min, 32 cycles of PCR stage at 95 °C for 45 *sec*, 65 °C for 1 min and 72 °C for 1 min	[35]
caspase 8	GAGCTGCTCTTCCGAATTA	GCAGGTTCATGTCATCATCC	hold stage at 95 °C for 3 min, 40 cycles of PCR stage at 95 °C for 15 *sec*, 61 °C for 20 *sec* and 72 °C for 30 *sec*	[36]
caspase 9	GAACTAACAGGCAAGCAGC	ACCTCACCAAATGCTCCAGAAC	Same as *caspase 3*	[34]
Smac/DIABLO	TGTGACGATTGGCTTTGGAGTAAC	TTCAATCAACGCATATGTGGTCTG	hold stage at 95 °C for 10 min, 50 cycles of PCR stage at 95 °C for 0 *sec*, 61 °C for 10 *sec* and 72 °C for 10 *sec*	[37]
β-actin	ACACTGTGCCCATCTACGAGGGG	ATGATGGAGTTGAAGGTAGTTTCGTGGAT		

(SF) was calculated as plating efficiency (PE) of treated sample/PE of control × 100, where PE equals number of colonies counted/ number of cells seeded × 100 [33].

2.7. Quantitative reverse transcription-polymerase chain reaction (qRT-PCR)

Total RNA from vehicle-treated control and CA-treated cells was isolated according the manufacture instructions (Total RNA Isolation System, Sigma-Aldrich). To determine the mRNA quantity of *caspase 3, caspase 4, caspase 8, caspase 9, smac/DIABLO*, quantitative real-time PCR (qRT-PCR) was used. After RNA extraction, cDNA was prepared using Power cDNA synthesis kit (iNtRON Biotechnology, South Korea). Amplification of target cDNA for apoptosis markers and *actin* (as a house keeping gene) was done using KAPA SYBR FAST qPCR Kit Master Mix (KAPA BIOSYSTEMS, USA) on Line Gene 9680 BioGR thermal cycler (Bioer Technology, USA). 5 μl of cDNA were mixed with 1 μl of forward primer (25X), 1 μl reverse primer (25X) (Table 1), 5.5 μl nuclease free water and 12.5 μl master mix. Each qRT- PCR reaction was run as triplicate for each primer pair (Table 1).

2.8. Cytochrome c release apoptosis assay

$5x10^7$ control and GI_{50}-treated cells were collected by centrifugation at 659 × g for 5 min, washed with ice cold PBS and centrifuged at 659 × g for 5 min, and re-suspended with 1X cytosolic extraction buffer mix containing dithiothreitol (DTT) and protease inhibitors. The cells were incubated on ice for 10 min, homogenized and centrifuged at 753 × *g* for 10 min. The supernatant was centrifuged again at 11,290 × *g* for 30 min to get the cytosolic fraction, while the pellet was re-suspended in mitochondrial extraction buffer to get mitochondrial fraction (Cytochrome *c* Release Apoptosis Assay Kit, Abcam, USA).

2.9. Western blot analysis

Control and GI_{50}-treated cells were washed 3 times with cold PBS and then lysed with protein lysis buffer [200 μl 10% sodium dodecyl sulfate (SDS), 10 μl 1 M Tris buffer pH 7.5, 10 μl 1 M sodium fluoride (NaF), 10 μl 1 M dithiothreitol (DTT), 20 μl 0.1 M ethylene glycol tetraacetic acid (EGTA) and 650 μl distilled water] on ice. The cell lysate was collected and heated for 5 min in boiling water bath and sonicated. Aliquots of lysates were diluted in 4x SDS-PAGE sample buffer (0.5 M Tris-HCl pH 6.8, 2% SDS, 20% glycerol, 20% 2-mercaptoethanol and 0.16% bromophenol blue) and proteins were resolved by electrophoresis on 10% or 12.5% SDS-polyacrylamide gels. Proteins transferred onto nitrocellulose membranes were blocked with 2% (w/v) BSA in Tris-buffered saline (TBS), and incubated overnight at 4 °C with primary antibodies: mouse monoclonal anti-β-actin (1:2000; Novus Biologicals, USA), mouse monoclonal anti-caspase 3 (1:500; Invitrogen, USA), rabbit polyclonal anti-caspase 4 (1:1000; Invitrogen, USA), mouse monoclonal anti-caspase 8 (1:1000; Invitrogen, USA), mouse monoclonal anti-caspase 9 (1:1000; Invitrogen, USA), mouse monoclonal anti-GAPDH (1:6000; CHEMICON, USA), rabbit monoclonal phospho-eukaryotic initiation factor-2 (p-EIF-2) (1:2000; Cell Signaling) and rabbit polyclonal anti-smac/DIABLO antibody (1:1000; R & D Systems, Germany) diluted in 1% BSA in TBS containing 0.05% Tween 20. After washing and incubation with appropriate secondary antibodies conjugated to IRDye 680 or 800 nm fluorescent dyes, the membranes were washed and the bands were visualized on FluorChem R system (Oxford, UK). Signals were quantified using AlphaView software (ProteinSimple, USA).

2.10. Statistical analysis

All experiments were performed with triplicate samples and repeated three times. Results are expressed as mean ± SEM. Statistical

analysis was performed using GraphPad Prism version 5.0 (GraphPad Software, San Diego, CA, USA). To determine differences between 3 or more means, one-way ANOVA with Fisher's LSD for multiple comparisons post-tests were performed. P value < 0.05 was considered significant.

3. Results

3.1. Purity and yield of cephalostatin analogues

The bis-steroidal diketone (compound **2**) is considered to be the cornerstone in our study. It can be synthesized in gram-scale starting from hecogenin acetate, a commercially available substance, using a seven-steps standard procedure with 35–38% overall yield [38]. Compound **2** underwent alkoxylation by oxidation of the enolate solution of **2** in the proper basic alcoholic solution using the mild oxidizing agent $PhI(OAc)_2$. The dimer **2** underwent a successful methoxylation reaction of C-11 using basic methanol yielding **3** as a pale yellow solid material in a recyclable process with 65% maximum yield. Similarly, the C_{11}-ethoxylated analogue **4** was generated as a white to pale yellow solid after oxidation of the ethanolic enolate solution of **2** with 70% maximum yield. The two analogues underwent a chemo and regioselective reduction reaction using excess sodium borohydride $NaBH_4$ reagent yielding the analogues **5** (CA5) and **6** (CA6) with excellent yield (90% and 95%, respectively) as a white solid material. However, when the enolate solution of **2** in isopropanol (i-PrOH) was oxidized using diacetoxy iodobenzene $PhI(OAc)_2$, a C_{11}-hydroxylation reaction instead of alkoxylation took place. This is rationalized basing on the slow and difficult attack of the bulky isopropoxide anion on the generated intermediate. Instead, the small hydroxide anion attacks the intermediate much faster and hence the C_{11}-OH analogue **7** is generated in a moderate yield (45%) as a white solid material (a mixture of 11α- and 11β-OH epimers). The isomeric mixture **7** underwent a sodium borohydride reduction yielding compound **8** as a white material in a good yield (65%). The reduction chemoselectivity mentioned in the previous cases (**5** and **6**) is lost here and hence both carbonyls at C-12 and C-12′ were reduced.

3.2. Compounds 5 and 6 (CA5, CA6) induce apoptosis in multiple cancer cell lines

The cytotoxicity of the six different cephalostatin analogues (CAs) was evaluated against three different human cancer cell lines (K-562, MCF-7 and DU-145). The corresponding GI_{50} (50% Growth Inhibition) and TGI (Total Growth Inhibition) values for each CA analogue are shown in Table 2. The results indicate that only compound **5** and compound **6** (CA5 and CA6) exhibit cytotoxic activities. Unless otherwise stated, the amounts of CA5 and CA6 used in subsequent experiments were the GI_{50} values from this table.

The cytotoxicity of CA5 and CA6 was attributed to the induction of apoptosis as indicated by nuclei fragmentation detected by fluorescence microscopy after DNA staining with DAPI (Fig. 1A) and by flow cytometry analysis of annexin V-FITC and PI staining (Fig. 1B). The cytotoxicity results at 24 h presented in Fig. 2A-B show that apoptosis induction by C5 and C6 occurred in a dose-dependent manner. In addition, the cytotoxicity of C5 and C6 was tested against human normal white blood cells (WBC) (Fig. 2C). Our results revealed that neither analogue had greater than 20% cytotoxicity in normal cells even after 72 h of treatment at the highest (10 μM) drug concentration tested (Fig. 2C). Thus, the cytotoxic effect of CA5 and CA6 is directed toward cancer cells.

Table 2
The MTT (3-(4,5-dimethylthiazol-2-yl)-2,5 diphenyltetrazolium bromide) assay results. a: 24 h, b: 48 h, c: 72 h.

CA	Cell line					
	K562		MCF-7		DU-145	
	GI50	TGI	GI50	TGI	GI50	TGI
Compound 3	X	X	X	X	X	X
Compound 4	X	X	X	X	X	X
Compound 5	0.014 μM[a]	9.3 μM[a]	0.03 μM[a]	4.8 μM[b]	0.82 μM[a]	8.9 μM[c]
Compound 6	0.061 μM[a]	1.2 μM[c]	0.11 μM[a]	X	0.37 μM[a]	X
Compound 7	X	X	X	X	X	X
Compound 8	X	X	X	X	X	X

3.3. Cephalostatin analogues (CAs) induce long-term cytotoxicity in cancer cell lines

To investigate the long-term cytotoxicity of compound **5** and compound **6**, in vitro clonogenic assay was performed [39]. The results presented in Fig. 3A-B show that cancer cell treatment with either CA5 or CA6 for 3 h followed by 12 days of culture resulted in a dose-dependent inhibition of clonogenic tumor growth (Fig. 3).

3.4. Caspase 3 and 9 mediate CA5 and CA6-induced apoptosis

qRT-PCR was used to measure the mRNA levels of apoptosis markers *caspase 3, caspase 8* and *caspase 9* in K-562, MCF-7 and DU-145 cells after treatment with CA5 or CA6 (Fig. 4A-B). *caspase 3* mRNA level increased in CA-treated K-562 and DU-145 cells when compared to vehicle-treated control cells. *Caspase 9* mRNA level increased in the three cell lines tested when compared to control cells. On the other hand, *caspase 8* mRNA level did not change significantly in CA-treated cells when compared to control untreated cells (Fig. 4A-B).

Moreover, treating cells with CA5 or CA6 resulted in activation of caspase 3 (cleavage of the procaspase to the active p17 form), and caspase 9 (cleavage of the procaspase to the active p35 and p37 forms) but not caspase 8 (no cleavage of the procaspase to the active p42 and p44 forms) (Fig. 4C). On the other hand, cells treated with etoposide (caspase-dependent drug) showed evidence of cleavage of procaspase 3, 9 and 8 to the active forms (Fig. 4C). The densitometry values (Fig. 4D) from the blots shown in Fig. 4C were normalized to actin or GAPDH and then expressed relative to the caspase pro- or cleaved form set at 1.0 in vehicle-treated control cells. To confirm the importance of caspase activation in CA5 and CA6-induced apoptosis, cells were pretreated with the pan caspase inhibitor (zVAD-fmk) (25 μM, 1 h) prior to treatment with CA5, CA6 or etoposide at the GI_{50} concentration. The results indicate that treated cells were protected from cytotoxicity (Fig. 4E).

3.5. C-11 functionalized cephalostatin 1 analogues treatment lead to apoptosis through the ER stress pathway

To test if the new cephalostatin analogues induce apoptosis in cancer cells in a similar manner to the 12′α-derivatives of cephalostatin 1 [28], we examined the activity of the endoplasmic reticulum stress pathway. Our results indicate that *smac/DIABLO* mRNA level increased in CA5- and CA6-treated K-562, DU-145 and MC-7 when compared to control cells (Fig. 5A). In addition, the results showed that treatment of cancer cell lines with CA5 or CA6 did not result in release of cytochrome *c* (CF fraction) from mitochondria (MF fraction), although the same cells treated with etoposide (caspase-dependent drug) as a positive control showed cytochrome *c* release (Fig. 5B and C). On the other hand, smac/DIABLO was released from mitochondria in cells treated with CA5, CA6 or etoposide (Fig. 5B and C).

Since compounds **5** and **6** induced caspase 9 activation and smac/DIABLO release and at the same time did not induce cytochrome *c* release or caspase 8 activation in cancer cells, we examined the phosphorylation of eIF-2, a target of ER stress that is initiated by thapsigargin, a well-characterized inducer of ER stress [40]. Treatment of the different cancer cell lines with CA5, CA6 or thapsigargin, induced an

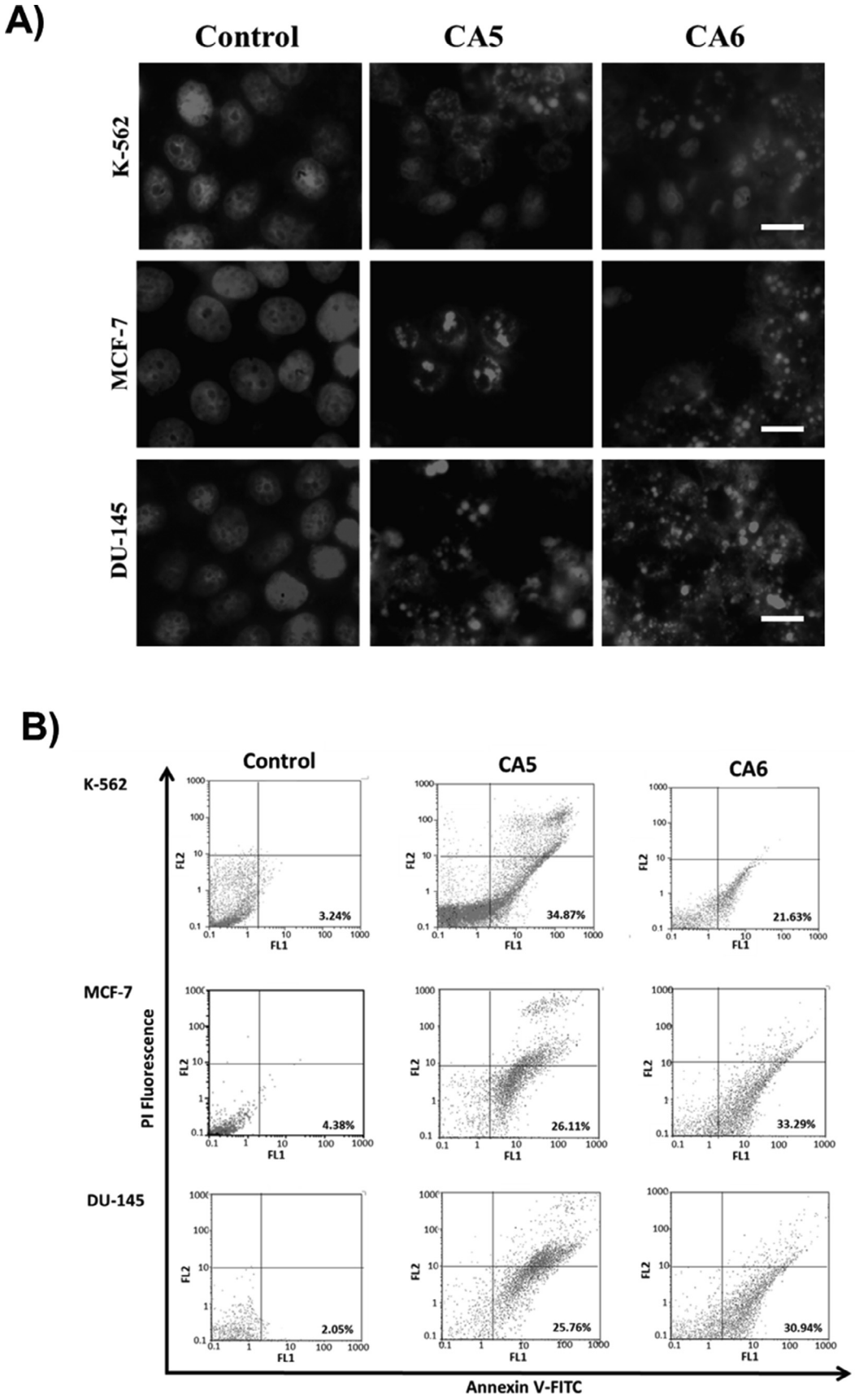

Fig. 1. Cephalostatin analogues compounds 5 and 6 (CA5 and CA6) induce apoptosis in cancer cells. Cells were treated for 24 h with CA5 or CA6 (GI50). A) Fluorescence images of tumor cell lines (K-562; MCF-7 and DU-145) showing fragmented nuclei after DAPI staining. Scale bar: 10 μm, B) Results from flow cytometry analysis of annexin V-FITC and PI-stained K-562, MCF-7 and DU-145 cells. Live cells (Annexin V negative, PI negative), apoptotic cells (Annexin V positive, PI negative) and necrotic cells (Annexin V positive, PI positive).

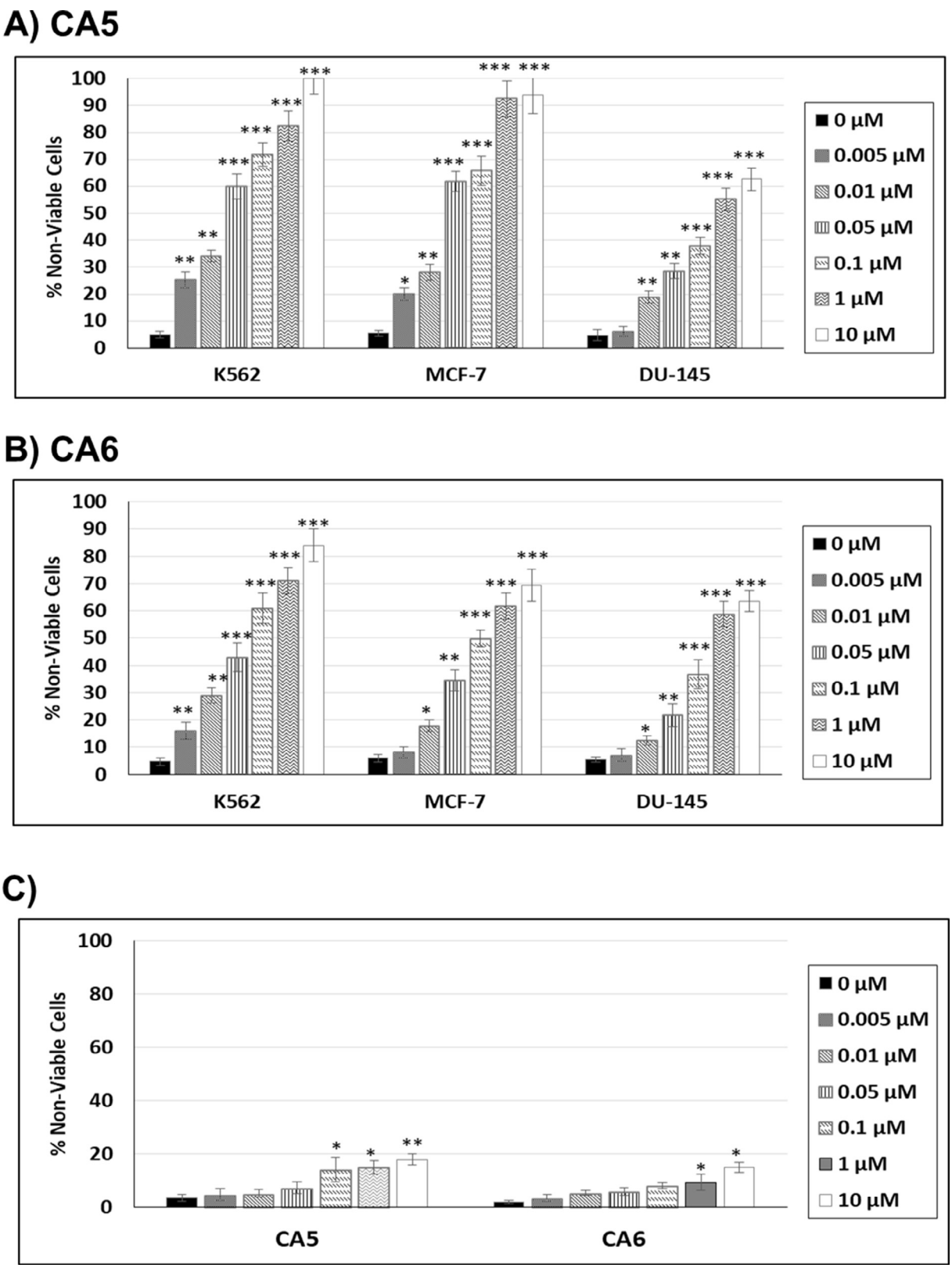

Fig. 2. CA5 and CA6-induced apoptosis is dose-dependent and cancer-specific. Cells were treated for 24 h with 10^4 range of concentrations of CA5 (A) or CA6 (B) and the percentage of non-viable cells was quantified. The percentage of non-viable cells relative to the vehicle-treated control cells measured by MTT assay, C) White blood cells were treated with 10^4 range of concentrations of CA5 or CA6 for 72 h and the percentage of non-viable cells was quantified. Percentage of non-viable cells relative to the vehicle-treated control cells is measured by MTT assay. Bars = mean ± S.E.M. of three independent experiments performed in triplicates.* $P < 0.05$; ** $P < 0.01$; *** $P < 0.001$ compared to vehicle-treated control cells.

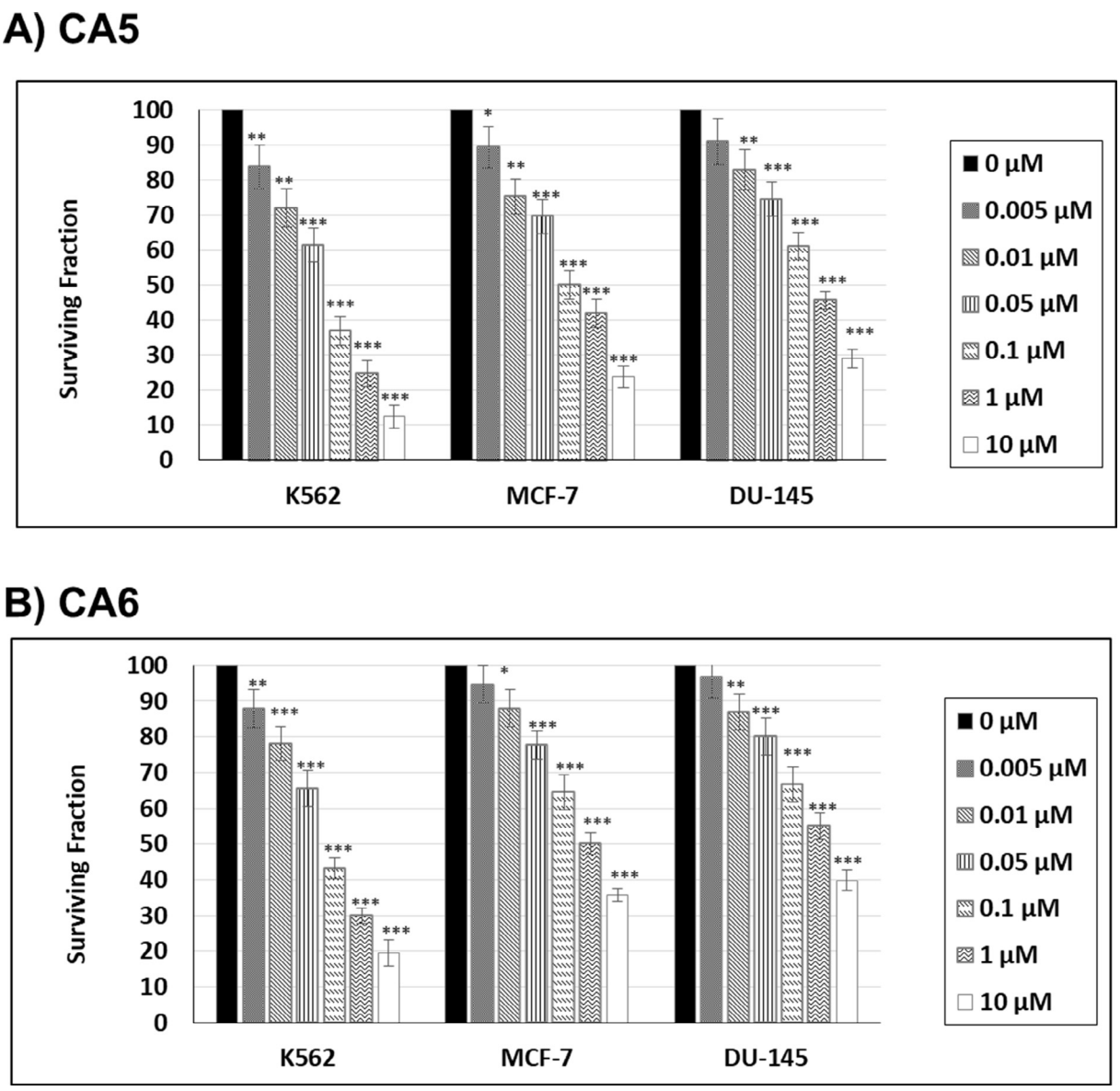

Fig. 3. Cephalostatin analogues CA5 and CA6 inhibit clonogenic tumor growth. Cells were treated for 3 h with 10^4 range of concentrations of CA5 (A) or CA6 (B) and the number of colonies was quantified after 12 days. Cephalostatin analogue treatment caused an inhibition of clonogenic tumor growth. Bars = mean ± S.E.M. of three independent experiments performed in duplicates. *P < 0.05; ** P < 0.01; *** P < 0.001 compared to vehicle-treated control cells.

increase in phospho-eIF-2 levels (Fig. 6A and B).

In addition, the mRNA quantity of caspase 4 (ER stress-specific caspase) [41,42] increased in all of the tested cell lines treated with CA5 and CA6 compared to vehicle-treated control cells (Fig. 6C). CA5, CA6 and thapsigargin treatment of K-562, MCF-7 and DU-145 cancer cells resulted in increased cleavage of caspase 4 (Fig. 6D and E). Furthermore, cells pretreated with the caspase 4 inhibitor Ac-LEVD-CHO (20 μM, 1 h) were protected from apoptosis induced by CA5 or CA6 (Fig. 6F).

Taken together, the results strongly suggest that the cephalostatin 1 C_{11}-functionalized analogues compound **5** and compound **6** induced apoptosis in K-562, MCF-7 and DU-145 cancer cells through the ER-mediated apoptotic pathway.

4. Discussion

Cephalostatin 1, which belongs to a twenty-membered family of cephalostatins, is well known for its efficient and remarkable cancer cells killing mechanism [24,25]. However, there are many limitations that reduce its utilization [25,43]. Cephalostatin 1 has an unusual structure with 13 rings formed by coupling of two different steroid units. In vitro synthesis of cephalostatin 1 is complicated and laborious; the synthesis of the two steroidal units required 68 steps with very low yield [43]. The combination of the collection difficulties and the synthesis complications, led to the synthesis of cephalostatin 1-related compounds (analogues) looking for utilizable alternatives to cephalostatin 1.

Even though none of the different cephalostatins contains a C-11O-functionalized group, we decide to synthesize such analogues to extract more information about the factors that could determine the biological activity of such class of compounds. Thus, this study was conducted to evaluate the cytotoxicity of six C-11 functionalized cephalostatin 1 analogues (Schemes 1, 2).

The cytotoxicity of the six cephalostatin 1 analogues was tested on three different cell lines: K-562 leukemia, MCF-7 breast cancer and DU 145 prostate cancer cell lines using the MTT test (Table 2). Compounds **5** and **6** (CA5 and CA6) showed a potent cytotoxic effect on the three cell lines tested, while the other analogues did not exhibit cytotoxic

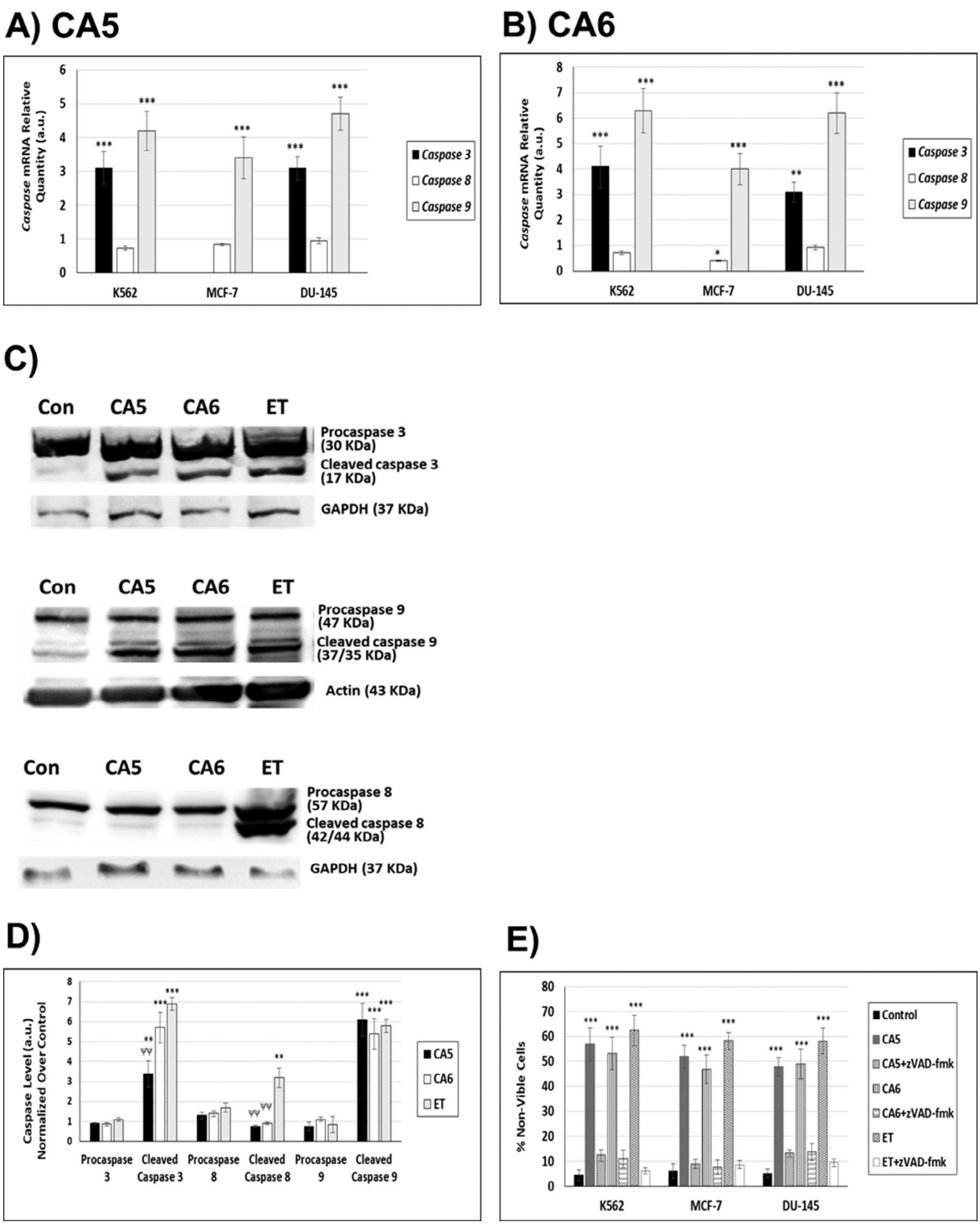

Fig. 4. CA5- and CA6-induced apoptosis is dependent on caspases activation. qRT-PCR analysis of *caspase 3*, *8* and *9* mRNA in CA5(A)- and CA6(B)-treated cells (GI50) as compared to vehicle-treated control cells [set as 1 arbitrary unit (a.u.)]. Note that MCF-7 cells do not express caspase 3. Values were normalized to *β-actin*, C) Representative Western blots showing cleavage "activation' of procaspase 3 to the active form p17, procaspase 9 to the active forms p35 and p37 and procaspase 8 to the active forms p42 and p44 in K562-treated cells (GI50). Etoposide (ET) was used (25 μg/ml, 24 h) as positive control (classical caspases-dependent inducer of apoptosis). Similar results were achieved in MCF-7 (except for caspase 3 activation) and DU-145 cancers cells. The experiment was repeated three times and the corresponding quantification is shown in (D), D) Quantification of procaspase 3, 8 and 9 and their cleaved forms in CA5-; CA6- and ET-treated K562 relative to the control values (set as 1.0) obtained from densitometers of immunoblots, E) Inhibition of CA5 and CA6-induced apoptosis by the pan caspase inhibitor zVAD-fmk. Cells were treated for 24 h with 0.1% DMSO (control), treated with CA5 or CA6 (GI50), or pretreated with zVAD-fmk (25 μM, 1 h) and then treated with CA5 or CA6. Percent non-viable cells: percentage of non-viable cells relative to the vehicle-treated control cells measured by MTT assay. Bars = mean ± S.E.M. of three independent experiments performed in triplicates. * $P < 0.05$; ** $P < 0.01$; *** $P < 0.001$ compared to vehicle-treated control cells, ψψ $P < 0.01$ compared to etoposide-treated cells.

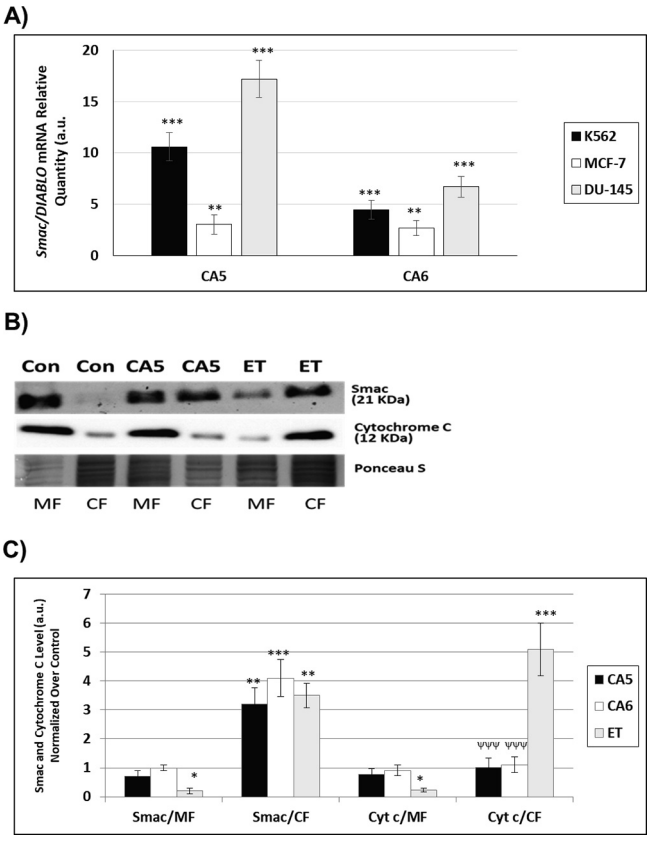

Fig. 5. CA5 and CA6 induce the release of smac/DIABLO but not cytochrome *c* from the mitochondria into the cytosol. A) qRT-PCR analysis of *smac/DIABLO* mRNA in CA5- and CA6-treated cells as compared to vehicle-treated control cells [set as 1 arbitrary unit (a.u.)]. Values were normalized to *β-actin*, B) Representative Western blot showing the release of smac/DIABLO but not cytochrome *c* from the mitochondria (MF) into the cytosol (CF) of treated K562 cancer cells (GI50). Similar results were achieved in MCF-7 and DU-145 cancer cells. Etoposide (ET) was used as a positive control (induces the translocation of both smac/DIABLO and cytochrome *c* from the mitochondria into the cytosol). Equal protein loading was controlled by staining membranes with Ponceau S (a representative section of the stained membrane is shown). The experiment was repeated three times and the corresponding quantification is shown in (C), C) Quantification of smac/DIABLO and cytochrome *C* levels in vehicle-treated control K562 cells and cells treated with GI_{50} amounts of CA5 and CA6 or etoposide as a positive control. Relative levels of smac/DIABLO and cytochrome *c* in treated cells compared to controls (set as 1.0) obtained from densitometry of immunoblots. MF: mitochondria fraction; CF: cytosol fraction. Bars = mean ± S.E.M. of three independent experiments performed in triplicates. *P < 0.05; ** P < 0.01; *** P < 0.001 compared to vehicle-treated control cells; ψψψ P < 0.001 compared to etoposide-treated cells.

effect within the measured concentrations. The rationale behind this could be that the presence of both 12′β-OH and 12-carbonyl groups is a requirement for the interaction between cephalostatin 1 or its analogues and the targeted proteins such as oxysterol binding protein (OSBP) and OSBP-related protein 4L (ORP4L) [44] or HSP70 isoform GRP78 [45], leading to the enhancement of the biological activity compared to that of the starting diketone **2**. Additionally, the presence of C_{11}-X group (X = OMe, OEt) in CA5 and CA6 enhanced the biological activity compared to the corresponding analogue with X = H. This may be due to the effect played by this functionality at this position on the polarity difference between the two halves of the bis-steroidal dimer leading to a polarity enhancement of the molecule which was hypothesized as a rationale for the biological activity [27,46].

From our data, it was noticed that compound **5** (R = Me) exerted better activity than **6** (R = Et), which may be rationalized based on relative bulkiness of the ethoxy group compared to the methoxy group which is more common in biologically active compounds. Noteworthy, none of the members of the cephalostatin family contains an ethoxy group. However, four out of the 20 cephalostatins contains methoxy group at position-1 or 1′. On the other hand, even though all cephalostatins contain several OH groups, compound **8** was found to be inactive in the measured range. This may be due to the absence of the neighboring carbonyl group at C-12 position. This seems to be a structural requirement along with 12′β-OH in the other half for a C_{11}-functionalized analogue to be active. This attracts us to synthesize more analogues with C_{11}-OH (with α- or β-configurations) holding the neighboring carbonyl and $C_{12'}$-OH groups.

CA5- and CA6-treated cells exhibited two features of apoptosis: fragmented nuclei and the externalization of phosphatidylserine. The latter was determined by annexin V binding [47] (Fig. 1A-B). In addition, their cytotoxicity was dose-dependent (Fig. 2A-B) and cancer cell-specific (Fig. 2C). Compound **5** and **6** apoptotic pathway(s) were studied using RT-PCR, Western blotting and cytochrome *c* and smac/DIABLO release from mitochondria (Figs. 3–6). Upon treatment with CA5 and CA6, caspase 3 and caspase 9 mRNA levels increased in the three cell lines (except for caspase 3 in MCF-7 cells) (Fig. 4A-B), whereas the mRNA level of caspase 8 did not change in any of the cell lines studied (Fig. 4A-B). In addition, the levels of active caspase 3 and 9 but not caspase 8 (cleaved caspase) were increased in the CA5- and CA6- treated cells (Fig. 4 C-D). Moreover, the cytotoxic effects of CA5 and CA6 were inhibited when the pan caspase inhibitor zVAD-fmk was used (Fig. 4 E). This confirms the involvement of caspase 3 and 9 in compound **5** and **6**-mediated apoptosis.

Since caspase 9 was mediating CA5 and CA6 cytotoxic activities, we tested whether this is through the mitochondria or ER apoptotic pathways. The results presented in Fig. 5A-C show that cytochrome *c* was not released from the mitochondria into the cytosol in the three cell lines tested upon treatment with CA5 or CA6. This indicates that the mitochondrial apoptotic pathway was not activated since this pathway needs the leakage of cytochrome *c* into cytosol to bind apaf-1 and procaspase 9 to form the apoptosome which ends in the activation of caspase 9 [9]. However, smac/DIABLO, a known inhibitor for inhibitors of apoptosis (IAPs) leading to caspases activation [48], was translocated from the mitochondria into the cytosol upon treatment. In addition, its mRNA level was increased when the cells were treated with either CA5 or CA6.

Additionally, the findings show that treating cells with CA5 or CA6 increased the level of phosphorylated eukaryotic translation initiation factor 2 (eIF2), an indicator of ER stress [12,14] (Fig. 6 A-B). In addition, the mRNA level of caspase 4 (the main player in ER-mediated apoptosis) as well as its cleaved active form were increased in cells treated with either CA5 or CA6 (Fig. 6 C-E). The activation of caspase 4 by CA5 and CA6 treatment was inhibited by caspase 4 specific inhibitor Ac-LEVD-CHO (Fig. 6F). These results suggest that CA5 and CA6 induce apoptosis through the ER-pathway similar to what was found for cephalostatin 1 [49] and the 12′α-derivatives of cephalostatin 1 [28].

In conclusion, treating cells with C_{11}-functionalized cephalostatin 1 analogues induced ER-stress which provided a pathway for the accumulation of smac/DIABLO. This in turn inhibited IAPs contributing to the activation of caspases including the ER-caspase 4 without cytochrome *c* release from mitochondria [12,15]. After being activated, caspase 4 activated caspase 9 which in turn activated caspase 3 ending in apoptosis [12,15]. The results presented in this work indicate that the C_{11}-functionalized analogues (CA5, CA6) induced apoptosis in a similar mechanism to cephalostatin 1 [16,18] and the 12′α-hydroxy derivatives of cephalostatin 1 [28], making them cephalostatin 1-utilizable alternatives.

Conflict of interest

The authors declare that they have no conflict of interest.

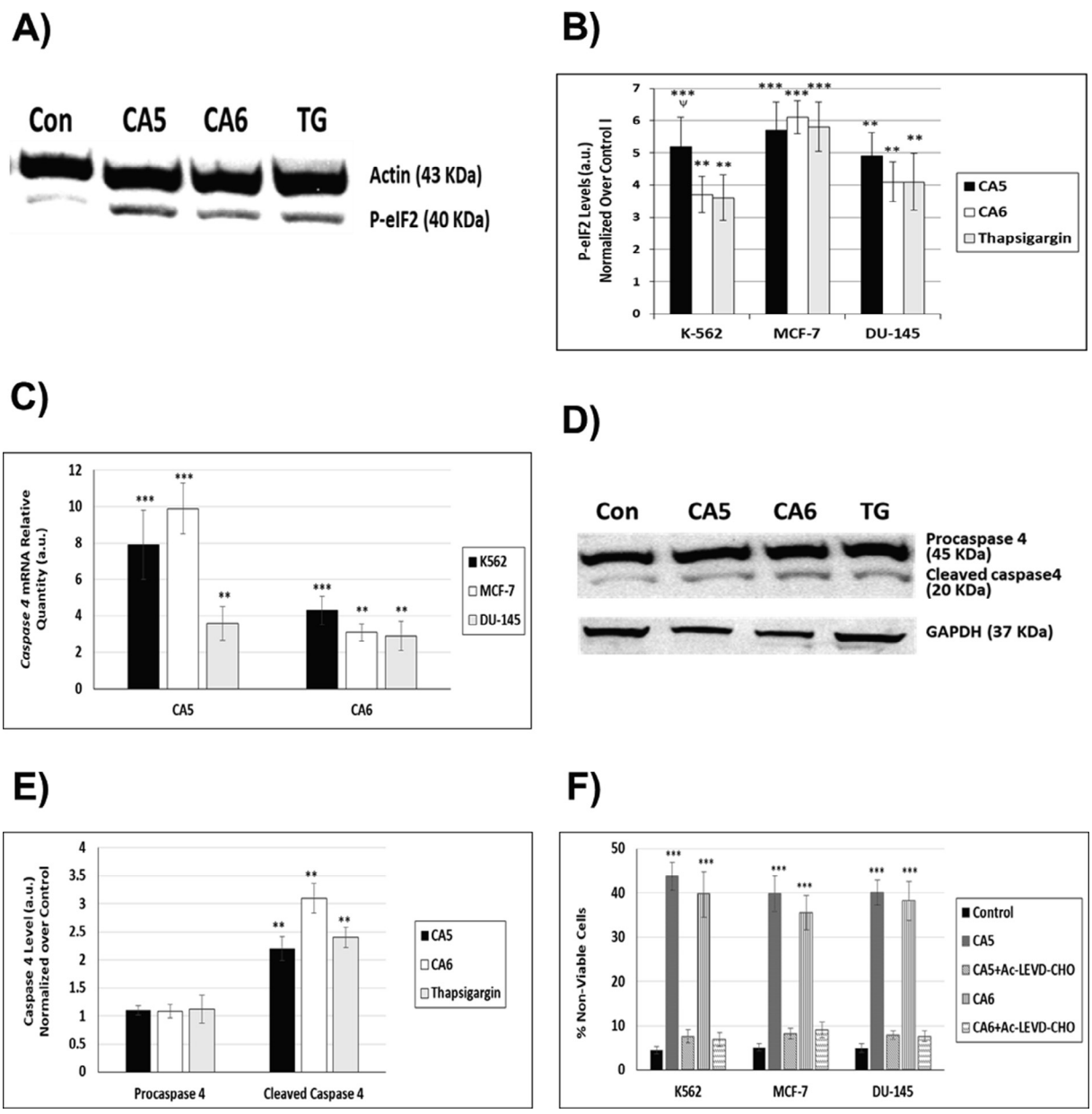

Fig. 6. CA5 and CA6 induce endoplasmic reticulum-mediated apoptosis. A) Representative Western blot showing the induction of phosphorylation of eukaryotic initiation factor-2 (eIF-2) in K562 cells treated with GI50 amounts of CA5 and CA6. For comparison purposes, thapsigargin (TG), an ER stress-causing drug was used (3 μM, 2 h) as a positive control. The experiment was repeated three times and the corresponding quantification is shown in (B), B) Quantification of PeIF-2 levels in CA5-, CA6- and thapsigargin-treated K-562; MCF-7 and DU-145 cells. Relative levels of PeIF-2 in treated cells compared to controls (set as 1.0) obtained from densitometry of immunoblots, C) qRT-PCR analysis of *caspase 4* mRNA in CA5- and CA6-treated cells as compared to vehicle-treated control cells [set as 1 arbitrary unit (a.u.)]. Values were normalized to *β-actin*, D) Representative Western blot showing cleavage "activation' of procaspase 4 to the active form p20 in K562 cancer cells. Similar results were achieved in MCF-7 and DU-145 cancers cells. The experiment was repeated three times and the corresponding quantification is shown in (E), E) Quantification of procaspase 4 and its cleaved form in CA5-; CA6- and TG-treated K562 relative to the control values (set as 1.0) obtained from densitometers of immunoblots, F) Inhibition of CA5 and CA6-induced apoptosis by the caspase 4-specific inhibitor Ac-LEVD-CHO. Cells were treated with 0.1% DMSO (control), treated with CA5 or CA6 (GI50), or pretreated with Ac-LEVD-CHO (20 μM, 1 h) and then treated with CA5 or CA6. Percent non-viable cells: percentage of non-viable cells relative to the vehicle-treated control cells measured by MTT assay. Bars = mean ± S.E.M. of three independent experiments performed in triplicates. ** $P < 0.01$; *** $P < 0.001$ compared to vehicle-treated control cells; ψ $P < 0.05$ compared to thapsigargin-treated cells.

Acknowledgement

This work was supported partially by The Deutsche Forschungsgemeinschaft (DFG). We gratefully acknowledge the support of the Deanship of Scientific Research, Al-Balqa Applied University. The authors are grateful to the Deanship of Scientific Research, the Hashemite University [grant number 75, 2018] for supporting the current work.

References

[1] X. Liang, C. Chen, Y. Zhao, P. Wang, Circumventing tumor resistance to chemotherapy by nanotechnology, Methods Mol. Biol. 596 (2010) 467–488.
[2] A. Florea, D. Büsselberg, Occurrence, use and potential toxic effects of metals and metal compounds, Biometals 19 (2006) 419–427.
[3] B. Baguley, D. Kerr, Y. Lu, R. Mahato, Anticancer drug development, Pharm. Persp. Cancer Therapeut. 8 (2001) 49–92.
[4] J. Felth, Studies of Cytotoxic Compounds of Natural Origin and Their Mechanism Of Action, PhD Thesis Uppsala University, Sweden, 2011, pp. 11–43.
[5] M. Mabunda, Synthesis and Biological Activity of Ajoenes with Increased Aqueous

Solubility, Ms Thesis University of Cape Town, South Africa, 2013, pp. 12–88.
[6] K. Masui, B. Gini, J. Wykosky, C. Zanca, P. Mischel, F. Furnari, W. Cavenee, A tale of two approaches: Complementary mechanisms of cytotoxic and targeted therapy resistance may inform next generation cancer treatments, Carcinogenesis 34 (2013) 725–738.
[7] Y. Liu, B. Levine, Autosis and autophagic cell death: The dark side of autophagy, Cell Death Differ. 22 (2014) 367–376.
[8] A. Parrish, C. Freel, S. Kornbluth, Cellular mechanisms controlling caspase activation and function, CSH Perspect. Biol. 5 (2013) 1–25.
[9] H. Hwang, H. Kim, Chondrocyte apoptosis in the pathogenesis of osteoarthritis, Int. J. Mol. Sci. 16 (2015) 26035–26054.
[10] H. Zou, R. Yang, J. Hao, J. Wang, C. Sun, S. Fesik, J. Wu, K. Tomaselli, R. Armstrong, Regulation of the Apaf-1/caspase-9 apoptosome by caspase-3 and XIAP, J. Biol. Chem. 278 (2003) 8091–8098.
[11] S. Fulda, K. Debatin, Extrinsic versus intrinsic apoptosis pathways in anticancer chemotherapy, Oncogene 25 (2006) 4798–4811.
[12] D. Breckenridge, M. Germain, J. Mathai, M. Nguyen, G. Shore, Regulation of apoptosis by endoplasmic reticulum pathways, Oncogene 22 (2003) 8608–8618.
[13] S. Logue, A. Gorman, P. Cleary, N. Keogh, A. Samali, Current concepts in ER stress-induced apoptosis, J. Carcinogene. Mutagene. S 6 (2013) 1–6.
[14] M. Cnop, S. Toivonen, M. Igoillo-Esteve, S. Paraskevi, Endoplasmic reticulum stress and eIF2α phosphorylation: The Achilles heel of pancreatic β cells, Mol. Metab. 6 (2017) 1024–1039.
[15] J. Groenendyk, M. Michalak, Endoplasmic reticulum quality control and apoptosis, Acta Biochim. Pol. 52 (2005) 381–395.
[16] V. Dirsch, I. Müller, S. Eichhorst, G. Pettit, Y. Kamano, M. Inoue, J. Xu, Y. Ichihara, G. Wanner, A. Vollmar, Cephalostatin 1 selectively triggers the release of Smac/DIABLO and subsequent apoptosis that is characterized by an increased density of the mitochondrial matrix, Cancer Res. 63 (2003) 8869–8876.
[17] V.M. Dirsch, A.M. Vollmar, Cephalostatin 1-induced apoptosis in tumor cells, in: M. Sluyser (Ed.), Application of Apoptosis to Cancer Treatment, Springer, Dordrecht, 2005, pp. 209–221.
[18] I. Müller, V. Dirsch, A. Rudy, A. Lopez, G. Pettit, A. Vollmar, Cephalostatin 1 inactivates Bcl-2 by hyperphosphorylation independent of m-phase arrest and DNA damage, Mol. Pharmacol. 67 (2005) 1684–1689.
[19] G. Pettit, M. Inoue, Y. Kamano, D. Herald, C. Arm, C. Dufresne, N. Christie, J. Schmidt, D. Doubek, T. Krupa, Isolation and structure of the powerful cell growth inhibitor cephalostatin 1, J. Am. Chem. Soc. 110 (1988) 2006–2007.
[20] Y. Li, J. Dias, Dimeric and oligomeric steroids, Chem. Rev. 97 (1997) 283–304.
[21] T.G. LaCour, C. Guo, S. Bhandaru, M.R. Boyd, P.L. Fuchs, Interphylal product splicing: The first total syntheses of cephalostatin 1, the north hemisphere ritterazine G, and the and the highly active hybrid analog, ritterostatin GNIN, J. Am. Chem. Soc. 120 (1998) 692.
[22] W. Li, T. LaCour, P. Fuchs, Dyotropic rearrangement facilitated proximal functionalization and oxidative removal of angular methyl groups: Efficient syntheses of 23'-deoxy cephalostatin 1 analogues 1, J. Am. Chem. Soc. 124 (2002) 4548–4549.
[23] W. Li, P. Fuchs, An efficient synthesis of the c-23 deoxy, 17α-hydroxy south 1 hemisphere and its cephalostatin 1 analog1, Org. Lett. 5 (2003) 2849–2852.
[24] G. Liebezeit, Aquaculture of “non-food organisms” for natural substance production, Adv. Biochem. Eng. Biotechnol. 97 (2005) 1–28.
[25] S. Lee, T. LaCour, P. Fuchs, Chemistry of trisdecacyclic pyrazine antineoplastics: The cephalostatins and ritterazines, Chem. Rev. 109 (2009) 2275–2314.
[26] J. Poza, J. Rodríguez, C. Jiménez, Synthesis of a new cytotoxic cephalostatin/ritterazine analogue from hecogenin and 22-epi-hippuristanol, Bioorg. Med. Chem. 18 (2010) 58–63.
[27] M.A. Iglesias-Arteaga, J.W. Morzycki, Cephalostatins and ritterazines, Alkaloids Chem. Biol. 72 (2013) 153–279.
[28] L.H. Tahtamouni, M.M. Nawasreh, Z.A. Al-Mazaydeh, R.A. Al-Khateeb, R.N. Abdellatif, R.M. Bawadi, J.R. Bamburg, S.R. Yasin, Cephalostatin 1 analogues activate apoptosis via the endoplasmic reticulum stress signaling pathway, Eur. J. Pharmacol. 818 (2018) 400–409.
[29] M. Nawasreh, Stereoselective Synthesis of Cephalostatin Analogues as Anticancer Agents, PhD Thesis Leibniz Hannover University, Germany, 2000.
[30] T. Mosmann, Rapid colorimetric assay for cellular growth and survival: Application to proliferation and cytotoxicity assays, J. Immunol. Methods 65 (1983) 55–63.
[31] A. Munshi, M. Hobbs, R.E. Meyn, Clonogenic cell survival assay, Methods Mol. Med. 110 (2005) 21–28.
[32] N.J. Sarma, A. Takeda, N.R. Yaseen, Colony forming cell (CFC) assay for human hematopoietic cells, J. Vis. Exp. 46 (2010) 2195.
[33] N.A. Franken, H.M. Rodermond, J. Stap, J. Haveman, C. van Bree, Clonogenic assay of cells in vitro, Nat. Protoc. 1 (2006) 2315–2319.
[34] W. Yaoxian, Y. Hui, Z. Yunyan, L. Yanqin, G. Xin, W. Xiaoke, Emodin induces apoptosis of human cervical cancer hela cells via intrinsic mitochondrial and extrinsic death receptor pathway, Cancer Cell Int. 13 (2013) 71.
[35] Z. Bian, S. Elner, V. Elner, Dual involvement of caspase-4 in inflammatory and ER stress-induced apoptotic responses in human retinal pigment epithelial cells, Investig. Ophthalmol. Vis. Sci. 50 (2009) 6006–6014.
[36] C. Van Geelen, B. Pennarun, B. Ek, P. Le, D. Spierings, E. De Vries, S. De Jong, Downregulation of active caspase 8 as a mechanism of acquired trail resistance in mismatch repair-proficient colon carcinoma cell lines, Int. J. Oncol. 37 (2010) 1031–1041.
[37] Y. Yan, C. Mahotka, S. Heikaus, T. Shibata, N. Wethkamp, J. Liebmann, C.V. Suschek, Y. Guo, H.E. Gabbert, C.D. Gerharz, Disturbed balance of expression between XIAP and Smac/DIABLO during tumour progression in renal cell carcinomas, Br. J. Cancer 91 (2004) 1349–1357.
[38] A. Kramer, U. Ullman, E. Winterfeldt, A short route to cephalostatin analogues, J. Chem. Soc. Perkin Trans. I (1993) 2865.
[39] V.N. Sumantran, Cellular chemosensitivity assays: an overview, Methods Mol. Biol. 731 (2011) 219–236.
[40] C.M. Oslowski, F. Urano, Measuring ER stress and the unfolded protein response using mammalian tissue culture system, Methods Enzymol. 490 (2011) 71–92.
[41] R. Bravo-Sagua, A.E. Rodriguez, J. Kuzmicic, T. Gutierrez, C. Lopez-Crisosto, C. Quiroga, J. Díaz-Elizondo, M. Chiong, T.G. Gillette, B.A. Rothermel, S. Lavandero, Cell death and survival through the endoplasmic reticulum-mitochondrial axis, Curr. Mol. Med. 13 (2013) 317–329.
[42] R. Iurlaro, C. Muñoz-Pinedo, Cell death induced by endoplasmic reticulum stress, FEBS J. 283 (2016) 2640–2652.
[43] A. Gryszkiewicz, I. Jastrzebska, J. Morzycki, D. Romanowska, Approaches towards the synthesis of cephalostatins, ritterazines and saponins from ornithogalum saundersiae-new natural products with cytostatic activity, Curr. Org. Chem. 7 (2003) 1257–1277.
[44] A.W. Burgett, T.B. Poulsen, K. Wangkanont, D.R. Anderson, C. Kikuchi, K. Shimada, S. Okubo, K.C. Fortner, Y. Mimaki, M. Kuroda, J.P. Murphy, D.J. Schwalb, E.C. Petrella, I. Cornella-Taracido, M. Schirle, J.A. Tallarico, M.D. Shair, Natural products reveal cancer cell dependence on oxysterol-binding proteins, Nat. Chem. Biol. 7 (2011) 639–647.
[45] A.J. Ambrose, E.A. Santos, P.C. Jimenez, D.D. Rocha, D.V. Wilke, P. Beuzer, J. Axelrod, A. Kumar Kanduluru, P.L. Fuchs, H. Cang, L.V. Costa-Lotufo, E. Chapman, J.J. La Clair, Ritterostatin $_{G}$N 1N, a cephalostatin-ritterazine bis-steroidal pyrazine hybrid, selectively targets GRP78, ChemBioChem 18 (2017) 506–510.
[46] C. Imperatore, A. Aiello, F. D'aniello, M. Senese, M. Menna, Alkaloids from marine invertebrates as important leads for anticancer drugs discovery and development, Molecules (2014) 20391–20423.
[47] E. Elmore, A. Jain, S. Siddiqui, N. Tohidian, F.L. Meyskens, V.E. Steele, J.L. Redpath, Development and characteristics of a human cell assay for screening agents for melanoma prevention, Melanoma Res. 17 (2007) 42–50.
[48] R.P. Rastogi, R.P. Sinha, Apoptosis: Molecular mechanisms and pathogenicity, EXCLI J. 8 (2009) 155–181.
[49] N. López, A. Rudy, N. Barth, L. Schmitz, G. Pettit, K. Schulze, V. Dirsch, A. Vollmar, The marine product cephalostatin 1 activates an endoplasmic reticulum stress-specific and apoptosome-independent apoptotic signaling pathway, J. Biol. Chem. 281 (2006) 33078–33086.